

Type-II Dirac nodal chain semimetal CrB_4

Xiao-Yao Hou(侯逍遥), Ze-Feng Gao(高泽峰), Peng-Jie Guo(郭朋杰), Jian-Feng Zhang(张建丰), and Zhong-Yi Lu(卢仲毅)

Citation: Chin. Phys. B, 2026, 35 (**1**): 017301. DOI: 10.1088/1674-1056/ae172b
http://cpb.iphy.ac.cn; http://iopscience.iop.org/cpb

What follows is a list of articles you may be interested in

A non-Hermitian approach for edge/surface states in bounded systems

Huiping Wang(王会平), Li Ren(任莉), Xiuli Zhang(张修丽), and Liguo Qin(秦立国)
Chin. Phys. B, 2025, 34 (**12**): 127304. DOI: 10.1088/1674-1056/ade1c1

Doping-induced magnetic and topological transitions in $Mn_2X_2Te_5$ (X = Bi, Sb) bilayers

Wei Chen(陈威), Chuhan Tang(唐楚涵), Chao-Fei Liu(刘超飞), and Mingxing Chen(陈明星)
Chin. Phys. B, 2025, 34 (**9**): 097304. DOI: 10.1088/1674-1056/ade4af

Random flux manipulating topological phase transitions in Chern insulators

Jinkun Wang(王锦坤) and Wu-Ming Liu(刘伍明)
Chin. Phys. B, 2025, 34 (**6**): 067301. DOI: 10.1088/1674-1056/adc36a

Merging and separation of polarization singularities in complex lattices

Mengyao Wang(王梦瑶), Tian Shi(石天), Luhui Ning(宁鲁慧), Peng Liu(刘鹏), Liangsheng Li(李粮生), and Ning Zheng(郑宁)
Chin. Phys. B, 2025, 34 (**3**): 037303. DOI: 10.1088/1674-1056/ada9da

Recent advances of defect-induced spin and valley polarized states in graphene

Yu Zhang(张钰), Liangguang Jia(贾亮广), Yaoyao Chen(陈瑶瑶), Lin He(何林), and Yeliang Wang(王业亮)
Chin. Phys. B, 2022, 31 (**8**): 087301. DOI: 10.1088/1674-1056/ac70c4

RAPID COMMUNICATION

Type-II Dirac nodal chain semimetal CrB_4

Xiao-Yao Hou(侯逍遥)[1,2,3], Ze-Feng Gao(高泽峰)[1,2], Peng-Jie Guo(郭朋杰)[1,2,†], Jian-Feng Zhang(张建丰)[4,‡], and Zhong-Yi Lu(卢仲毅)[1,2,5,§]

[1] *School of Physics and Beijing Key Laboratory of Opto-electronic Functional Materials & Micro-nano Devices. Renmin University of China, Beijing* 100872, *China*

[2] *Key Laboratory of Quantum State Construction and Manipulation (Ministry of Education), Renmin University of China, Beijing* 100872, *China*

[3] *School of Physics and Engineering, Henan University of Science and Technology, Luoyang* 471023, *China*

[4] *Center for High Pressure Science & Technology Advanced Research, Beijing* 100094, *China*

[5] *Hefei National Laboratory, Hefei* 230088, *China*

(Received 23 September 2025; revised manuscript received 17 October 2025; accepted manuscript online 24 October 2025)

Dirac nodal line semimetals with topologically protected drumhead surface states have attracted intense theoretical and experimental attention over a decade. However, the study of type-II Dirac nodal line semimetals is rare, especially the type-II nodal chain semimetals have not been confirmed by experiment due to the lack of ideal material platform. In this study, based on symmetry analysis and the first-principles electronic structure calculations, we predict that CrB_4 is an ideal type-II Dirac nodal chain semimetal protected by the mirror symmetry. Moreover, there are two nodal rings protected by both space-inversion and time-reversal symmetries in CrB_4. More importantly, in CrB_4 the topologically protected drumhead surface states span the entire Brillouin zone at the Fermi level. Considering the fact that CrB_4 has been synthesized experimentally and the spin–orbit coupling is very weak, CrB_4 provides an ideal material platform for studying the exotic properties of type-II Dirac nodal chain semimetals in experiment.

Keywords: type-II nodal chain semimetal, nontrivial surface states, weak spin–orbit coupling

PACS: 73.20.At, 71.20.–b, 71.90.+q, 75.70.Tj

DOI: 10.1088/1674-1056/ae172b **CSTR:** 32038.14.CPB.ae172b

1. Introduction

Topological semimetals with symmetry-protected band crossing have attracted intense theoretical and experimental interest due to numerous novel physical properties, such as topologically protected boundary states, chiral anomaly, chiral zero sound, large magnetoresistance effect, and topological catalysis.[1–6] According to both the degeneracy and dimension of band crossing, topological semimetals are divided into zero-dimensional Weyl semimetals,[7,8] Dirac semimetals,[9–12] triple degenerate semimetals,[13–16] sixfold degenerate semimetals,[13,17,18] eightfold degenerate semimetals,[13,19,20] one-dimensional nodal-line semimetals,[21–23] and two-dimensional nodal surface semimetals.[24–27] On the other hand, based on whether the zero-dimensional band crossing has a strong tilt along a certain direction, zero-dimensional topological semimetals can also be divided into type-I and type-II topological semimetals, such as type-II Weyl semimetals.[28–30] In comparison, type-II topological semimetals have unique physical properties different from type-I topological semimetals such as angle-dependent chiral anomaly and topological Lifshitz transitions.[28–30]

One-dimensional nodal line semimetals are divided into Dirac and Weyl nodal line semimetals.[21–23] Moreover, multiple nodal lines can also form nodal chain semimetals, hopf-links nodal line semimetals and so on.[31,32] Naturally, the band crossing on the nodal lines can contain type-II Dirac and Weyl points, and the corresponding topological semimetals are called type-II Dirac and Weyl nodal line semimetals, respectively. Although several type-I nodal line and nodal chain semimetals have been experimentally confirmed,[33–35] type-II nodal line semimetals have rarely been experimentally confirmed due to the lack of an ideal material platform. Until recently, ZrSiSe was confirmed as a type-II nodal line semimetal by angle-resolved photoemission spectroscopy (ARPES) measurement.[36] However, type-II nodal chain semimetals have not yet been experimentally confirmed. Therefore, it is very meaningful to predict type-II nodal chain semimetals with distinct properties for the study of their novel physical properties in experiment.

In this study, based on symmetry analysis and the first-principles electronic structure calculations, we predict that CrB_4 is an ideal type-II Dirac nodal chain topological

†Corresponding author. E-mail: guopengjie@ruc.edu.cn

‡Corresponding author. E-mail: jianfeng.zhang@hpstar.ac.cn

§Corresponding author. E-mail: zlu@ruc.edu.cn

© 2026 Chinese Physical Society and IOP Publishing Ltd. All rights, including for text and data mining, AI training, and similar technologies, are reserved.

semimetal protected by the mirrors M_z and M_y (1/2, 1/2, 1/2). In addition, there are also two nodal rings protected by both space-inversion (I) and time-reversal (T) symmetries. More importantly, the topologically protected Fermi arcs of CrB_4 at the Fermi level span the entire Brillouin zone. When spin–orbit coupling (SOC) is considered, CrB_4 transforms from type-II nodal chain semimetal to strong topological insulator with Z_2 topological invariant (1,000).

2. Method

The structural optimization and electronic structure calculation of CrB_4 were studied in the framework of density functional theory (DFT)[37,38] in the Vienna *ab initio* simulation package (VASP).[39–41] The core electrons as well as the interaction between the core and valence electrons were described by using the projector augmented-wave meth.[42] The generalized gradient approximation (GGA) of Perdew–Burke–Ernzerhof (PBE)[43] type was treated with exchange–correlation functional, using an energy cut-off of 600 eV for the plane waves. A $14 \times 16 \times 20$ Monkhorst–Pack k mesh was used for the Brillouin zone sampling of the unit cell. The internal atomic positions were fully relaxed until the forces on all atoms were smaller than 0.01 eV/Å. The tight-binding Hamiltonian was constructed by the maximally localized Wannier functions[44–46] and the corresponding topological properties were obtained by using the WannierTools package.[47]

3. Results

Chromium tetraboride (CrB_4), originally suggested to have the *Immm* space group (No. 71) with the *oI*10 unit cell in Pearson notation, was known for its excellent adhesive wear resistance due to its high hardness.[48] Afterwards, Niu *et al.*[49] experimentally confirmed the existence of orthorhombic space group *Pnnm* (No. 58) CrB_4 with *op*10 unit cell in Pearson notation, which has a lower symmetry than the former. We optimize the experimental structure for CrB_4 with the orthorhombic *Pnnm* space group. The optimized lattice constants are $a = 4.72$ Å, $b = 5.47$ Å, and $c = 2.85$ Å. Due to the strong correlation of 3d-orbital electrons, CrB_4 may have magnetism. We consider different magnetic structures for CrB_4, all of which are optimized to nonmagnetic states. CrB_4 is thus a paramagnetic material, which is consistent with the experimental results.[48] The crystal structure of CrB_4 is shown in Figs. 1(a)–1(c). From the a direction, CrB_4 is composed of the Cr atomic layer and the B atomic layer, while the B atomic layer is formed by the distorted hexagons of B atoms (Figs. 1(a) and 1(c)), which results in the low symmetry of CrB_4. The point group symmetry of CrB_4 is D_{2h} with generator elements C_{2z}, C_{2x} (1/2, 1/2, 1/2) and I. The bulk and surface Brillouin zone (BZ) with the high-symmetry points and lines are shown in Fig. 1(d).

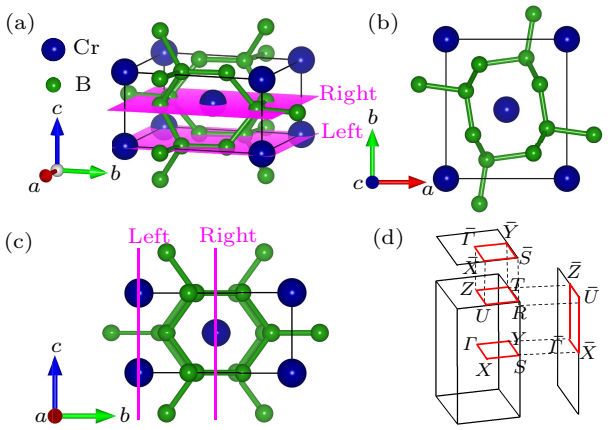


Fig. 1. (a)–(c) The crystal structures of CrB_4 with side view, top view along the c and a directions, respectively. The magenta planes and lines represent the corresponding left and right terminations. (d) Bulk, (001), and (010) projected 2D surface BZs of CrB_4, where the high-symmetry lines and the high-symmetry points are marked.

To study the topological properties of CrB_4, we calculate its electronic band structure along the high-symmetry directions without SOC, which is shown in Fig. 2(a). From Fig. 2(a), CrB_4 is a semimetal and has only blue and yellow bands crossing the Fermi level. Moreover, there are band crossings around the Fermi level, thus CrB_4 may be topological semimetal protected by crystal symmetry. Symmetry analysis indicates the band crossing points at the Γ–X and Γ–Y axes are protected by the M_z symmetry. Due to the strong tilt along the Γ–X direction, the crossing point is a type-II Dirac point. The crossing point on the Γ–Y axis is not tilted along the Γ–Y direction and is therefore a type-I Dirac point. Since the band crossing points on the different directions can lead to a nodal ring, CrB_4 has a nodal ring with both type-I and type-II Dirac points protected by the M_z symmetry. In addition, there is another band crossing in the Γ–X direction protected by M_y(1/2, 1/2, 1/2) symmetry, which is marked by a red arrow. We guess that there may be two small nodal rings in the $k_y = 0$ plane protected by the M_y(1/2, 1/2, 1/2) symmetry. To prove our guess, we calculate all the nodes for the blue and yellow bands in the entire BZ, which is shown in Fig. 2(c). As guessed, CrB_4 has indeed two small nodal rings in the $k_y = 0$ plane protected by M_y(1/2, 1/2, 1/2) symmetry (Fig. 2(c)). Since the two small nodal rings have a crossing with a larger nodal ring (Fig. 2(c)), CrB_4 is a topological nodal chain semimetal. Besides the nodal chain, there are also two nodal rings located in the non-high-symmetry surface of the BZ, which can be connected by the mirror M_z. The two nodal rings located in the non-high-symmetry surface of BZ are only protected by the IT symmetry (the T represents the time-reversal symmetry and I represents the space-reversal symmetry). In order to show the nodal ring of CrB_4 more directly, we also calculate the three-dimensional diagram of the yellow and blue bands. From Fig. 2(b), the nodal ring in the $M_z = 0$ plane has relatively large dispersion and the type-I

Dirac points below the Fermi level are clearly shown, which is conducive to observation by the ARPES experiment. Therefore, CrB_4 is an ideal Dirac nodal chain topological semimetal.

Then, we also calculate the three-dimensional Fermi surface of the CrB_4, which is shown in Fig. 2(d). From Fig. 2(d), CrB_4 has a hole-type Fermi surface (blue) and an electron-type Fermi surface (yellow). Moreover, our calculations show that the volume of the hole Fermi surface is equal to that of the electron Fermi surface, which results in the compensation of the hole and electron carriers.[50,51]

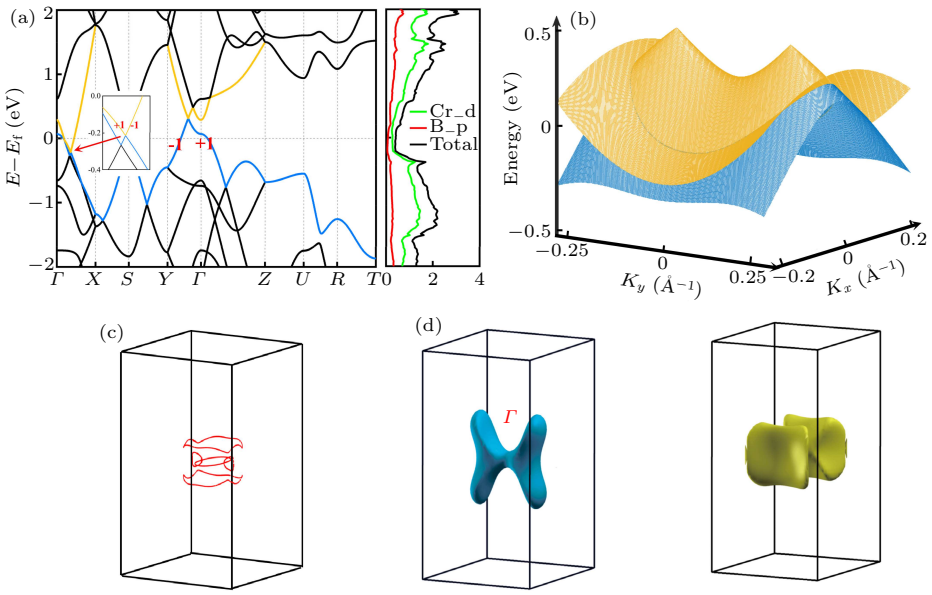


Fig. 2. (a) The band structure along high-symmetry directions (left panel) and density of states (right panel) for CrB_4 without SOC. The +1 and −1 are the eigenvalues of the mirror M_z. (b). Bulk energy dispersions of highest valence (bule) and lowest conduction (yellow) bands in the $k_z = 0$ plane. (c) The nodal rings and chain in the BZ for CrB_4. (d) The hole-type (left panel) and electron-type (right panel) Fermi surfaces.

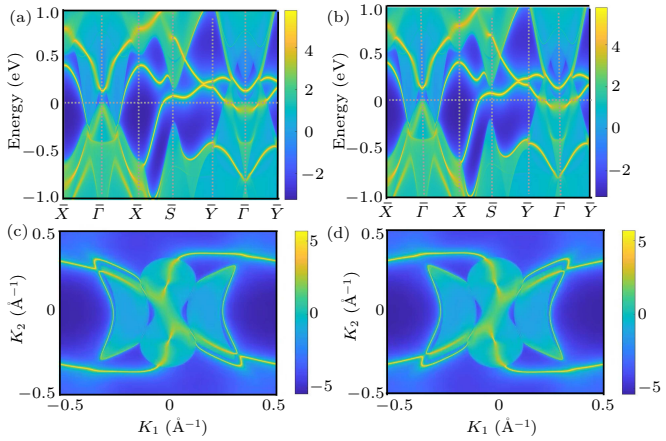


Fig. 3. Spectral function along the high-symmetry directions of CrB_4 left (a) and right (b) terminations for the (001) surface, which are contributed by Cr–B layers. The Fermi arcs at the Fermi level for left (c) and right (d) terminations.

It is well known that nodal ring semimetals have topologically protected boundary states. CrB_4 has five nodal rings which can be projected onto the (001) and (010) surfaces (Fig. 2(c)). Therefore, CrB_4 has topologically protected boundary states on both (001) and (010) surfaces. Then, we calculate the boundary states of CrB_4 on the (001) and (010) surfaces, which are shown in Figs. 3 and 4, respectively. For the (001) surface, CrB_4 has three topologically protected surface states crossing the Fermi level deriving from the three nodal rings projected onto the (001) surface. More importantly, the Fermi arcs of CrB_4 at the Fermi level span the entire BZ. For the (010) surface, CrB_4 has two topologically protected surface states near the Fermi level deriving from two small nodal rings projected onto the (010) surface. Moreover, the Fermi arcs at the Fermi level also span the entire BZ. The Fermi arcs across the entire BZ at the Fermi level may result in CrB_4 having good catalytic property.[5,6]

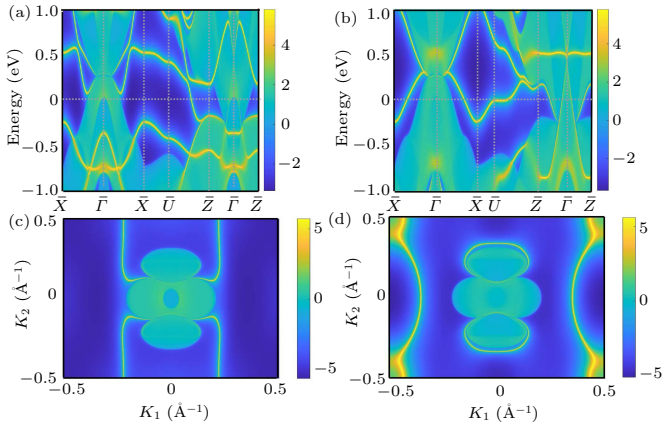


Fig. 4. Spectral function along the high-symmetry directions of CrB_4 left (a) and right (b) terminations for the (010) surface, which are contributed by B layers. The Fermi arcs at the Fermi level for left (c) and right (d) terminations.

When considering SOC, the symmetry of CrB_4 changes from D_{2h} point group to D_{2h} double point group. The highest symmetry for the high-symmetry axis in the BZ is C_{2v} double group, such as the Γ–X axis. Since there is only one two-dimensional irreducible representation for C_{2v} double group,

both the nodal rings and nodal chain of CrB_4 must open an energy gap. Since both B and Cr atoms are light elements, the SOC effect of CrB_4 is very weak. With SOC (as shown in Fig. 6), the sizes of the open bandgaps at the Γ–X and Γ–Y Dirac points are 2 meV, 27 meV, and 18 meV, respectively, for CrB_4 (Fig. 5(a)). Considering that the SOC effect of the 2p orbitals of a B atom is much smaller than 1 meV, the four bands near the Fermi level are mainly contributed by the 3d orbitals of the Cr atom, which is also proved by the calculation of the DOS of CrB_4 (Fig. 2(a)). Due to the weak SOC effect, CrB_4 can be a model material for studying the novel physical properties of the type-II Dirac nodal chain in experiment.

On the other hand, what topological phase will CrB_4 transition into from Dirac nodal chain semimetal under SOC? Since the parities of the two inversion bands at the time-reversal invariant Γ point are opposite (Fig. 5(a)), CrB_4 may be a strong topological insulator. In order to determine the Z_2 topological invariants of CrB_4, we need to calculate the parities of the eight time-reversal invariant points for 48 bands below the yellow bands.[52]

$$\begin{aligned}(x,y,z) &\xrightarrow{C_{2x}(\frac{1}{2},\frac{1}{2},\frac{1}{2})} \left(x+\frac{1}{2},-y+\frac{1}{2},-z+\frac{1}{2}\right)\\ &\xrightarrow{I} \left(-x-\frac{1}{2},y-\frac{1}{2},z-\frac{1}{2}\right), \qquad (1)\\ (x,y,z) &\xrightarrow{I} (-x,-y,-z)\\ &\xrightarrow{C_{2x}(\frac{1}{2},\frac{1}{2},\frac{1}{2})} \left(-x+\frac{1}{2},y+\frac{1}{2},z+\frac{1}{2}\right). \qquad (2)\end{aligned}$$

In fact, the nonsymmorphic symmetry of CrB_4 can greatly simplify the calculation of Z_2 topological invariants. The SOC effect does not change the parity of time-reversal invariant points, thus we only need to perform symmetry analysis without SOC. According to Eqs. (1) and (2), $C_{2x}(1/2,1/2,1/2)I = IC_{2x}(1/2,1/2,1/2)\,e^{-ikT}$, where T represents the translation (1,1,1). Obviously, the fractional translation (1/2, 1/2, 1/2) makes C_{2x} and I anticommutative at the time-reversal invariant X, Y, Z, and R points. Suppose Ψ is an eigenstate of I with eigenvalue to be 1. Since $C_{2x}(1/2,1/2,1/2)$ and I are anticommutative, $C_{2x}(1/2,1/2,1/2)\Psi$ is eigenstate of I with eigenvalue to be -1. Moreover, the Hamiltonian of CrB_4 commutes with $C_{2x}(1/2,1/2,1/2)$ and I, so Ψ and $C_{2x}(1/2,1/2,1/2)\Psi$ form a double degenerate state at time-reversal invariant X, Y, Z, and R points as shown in Fig. 2(a). Since the symmetry analysis is general, every band has double degeneracy at the time-reversal invariant X, Y, Z, and R points, and the parity product of every doubly degenerate band is -1. There are 12 doubly degenerate bands below the yellow band, so the parity product of the occupying states at the time-reversal invariant points X, Y, Z and R is 1.

Similar to the time-reversal invariant X, Y, Z and R points, our analysis indicates the $C_{2x}(1/2,1/2,1/2)$ and M_z being anticommutative at the time-reversal invariant U and T points. If Ψ is the eigenstate of M_z with the eigenvalue 1, $C_{2x}(1/2,1/2,1/2)\Psi$ is the eigenstate of M_z with the eigenvalue -1. The Hamiltonian of CrB_4 is commutative with both $C_{2x}(1/2,1/2,1/2)$ and M_z, so Ψ and $C_{2x}(1/2,1/2,1/2)\Psi$ form a doubly degenerate state. Given that I is also commutative with both $C_{2x}(1/2,1/2,1/2)$ and M_z, Ψ and $C_{2x}(1/2,1/2,1/2)\Psi$ have the same parity. Since every band has double degeneracy at the time-reversal invariant U and T points, and the parity product of every doubly degenerate band is 1, the product of the parity of the time-reversal invariant U and T points is 1 for the 12 doubly degenerate bands below the yellow band.

For the time-reversal invariant S point, $(C_{2x}(1/2,1/2,1/2)T)^2$ is equal to -1, which causes Ψ and $C_{2x}(1/2,1/2,1/2)T\Psi$ to become Kramers degenerate. Since $C_{2x}(1/2,1/2,1/2)T$ and I are commutative, the product of parity of every degenerate state at the time-reversal invariant S point is 1. Correspondingly, the product of parity at the time-reversal invariant S point is also 1 for the 12 doubly degenerate bands below the yellow band. These results from the above symmetry analysis are shown in Table 1. Thus the Z_2 topological invariant of CrB_4 depends only on the parity of the Γ point. Our calculations show that the product of parity at the time-reversal invariant Γ point for the 24 non-degenerate bands below the yellow band is -1 (Table 1). When SOC is considered, the 24 bands below the yellow band become 48 bands. However, the calculation of the Z_2 topological invariants requires only the product of the parity of half of the 48 bands, which is consistent with the result of the parity product of the 24 bands without SOC. According to these results in Table 1, the Z_2 topological invariants are (1,000) for CrB_4, which is also consistent with calculations of WannierTools packages. Therefore, CrB_4 is a strong topological insulator.

Table 1. The product of parity of eight time-reversal-invariant points (TRTPs) for the 24 bands below the yellow band.

TRIPs	Γ	Z	U	R	T	X	Y	S	Total
Parity	−	+	+	+	+	+	+	+	−

The strong topological insulator has nontrivial Dirac surface states protected by the time-reversal symmetry. The calculated topological surface states of CrB_4 on the (001) surface are shown in Fig. 5(b). Compared with Fig. 3(a), one topologically protected surface state splits into two, but the splits are very small, so the Dirac points of the surface state protected by the time-reversal symmetry are not obvious, which also implies the weak SOC effect of CrB_4. Since there are only two nontrivial bands around the Fermi level and its topologically protected surface states at the Fermi level span the entire BZ, CrB_4 is an ideal type-II Dirac nodal chain semimetal with distinct properties.

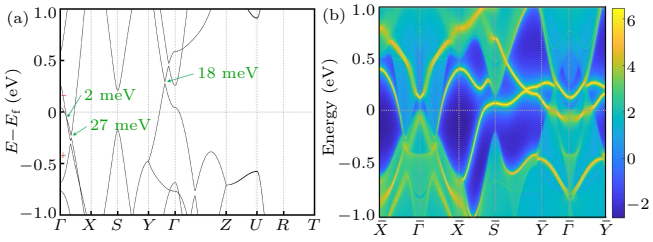


Fig. 5. (a) The band structure for CrB_4 with SOC along high-symmetry directions. (b) Spectral function along the high-symmetry directions left terminations for the (001) surface. The '+' and '−' represent parity for space-inversion symmetry.

4. Summary

Based on symmetry analysis and the first-principles electronic structure calculations, we predict that CrB_4 is a topological semimetal with a type-II nodal chain and two nodal rings protected respectively by mirror symmetry and *IT* symmetry. More importantly, the topologically protected drumhead surface states of CrB_4 span the entire BZ at the Fermi level. Meanwhile, there are only two nontrivial bands crossing the Fermi level, thus CrB_4 is an ideal type-II Dirac nodal chain semimetal with distinct properties. When considering SOC, CrB_4 transforms from topological semimetal phase to topological insulator phase. Because it has been synthesized experimentally and has a very weak SOC effect, CrB_4 is an ideal material platform for studying the exotic properties of type-II Dirac nodal chain semimetals in experiment.

Acknowledgements

This work was financially supported by the National Natural Science Foundation of China (Grant Nos. 12434009, 12204533, 62476278, and 62206299), the National Key R&D Program of China (Grant No. 2024YFA1408601), the Fundamental Research Funds for the Central Universities, the Research Funds of Renmin University of China (Grant No. 24XNKJ15), and the Innovation Program for Quantum Science and Technology (Grant No. 2021ZD0302402). Computational resources have been provided by the Physical Laboratory of High Performance Computing at Renmin University of China.

References

[1] Weng H, Dai X and Fang Z 2016 *J. Phys. Condens. Matter* **28** 303001
[2] Bernevig A, Weng H, Fang Z and Dai X 2018 *J. Phys. Soc. Jpn.* **87** 041001
[3] Zou J, He Z and Xu G 2019 *npj Comput. Mater.* **5** 96
[4] Lv B Q, Qian T and Ding H 2021 *Rev. Mod. Phys.* **93** 025002
[5] Li G and Felser C 2020 *Appl. Phys. Lett.* **116** 070501
[6] Xie R, Zhang T, Weng H and Chai G L 2022 *Small. Sci.* **2** 2100106
[7] Wan X, Turner A M, Vishwanath A and Savrasov S Y 2011 *Phys. Rev. B* **83** 205101
[8] Weng H, Fang C, Fang Z, Bernevig B A and Dai X 2015 *Phys. Rev. X* **5** 011029
[9] Young S M, Zaheer S, Teo J C Y, Kane C L, Mele E J and Rappe A M 2012 *Phys. Rev. Lett.* **108** 140405
[10] Wang Z, Sun Y, Chen X Q, Franchini C, Xu G, Weng H, Dai X and Fang Z 2012 *Phys. Rev. B* **85** 195320
[11] Wang Z, Weng H, Wu Q, Dai X and Fang Z 2013 *Phys. Rev. B* **88** 125427
[12] Liu Z K, Zhou B, Zhang Y, Wang Z J, Weng H M, Prabhakaran D, Mo S K, Shen Z X, Fang Z, Dai X, Hussain Z and Chen Y L 2014 *Science* **343** 864
[13] Bradlyn B, Cano J, Wang Z, Vergniory M G, Felser C, Cava R J and Bernevig B A 2016 *Science* **353** aaf5037
[14] Weng H, Fang C, Fang Z and Dai X 2016 *Phys. Rev. B* **93** 241202
[15] Zhu Z, Winkler G W, Wu Q, Li J and Soluyanov A A 2016 *Phys. Rev. X* **6** 031003
[16] Guo P J, Yang H C, Liu K and Lu Z Y 2018 *Phys. Rev. B* **98** 045134
[17] Kumar N, Yao M, Nayak J, *et al.* 2020 *Adv. Mater.* **32** 1906046
[18] Yáng X, Cochran T A, Chapai R, *et al.* 2020 *Phys. Rev. B* **101** 201105
[19] Wieder B J, Kim Y, Rappe A M and Kane C L 2016 *Phys. Rev. Lett.* **116** 186402
[20] Guo P J, Wei Y W, Liu K, Liu Z X and Lu Z Y 2021 *Phys. Rev. Lett.* **127** 176401
[21] Burkov A A, Hook M D and Balents L 2011 *Phys. Rev. B* **84** 235126
[22] Weng H, Liang Y, Xu Q, Yu R, Fang Z, Dai X and Kawazoe Y 2015 *Phys. Rev. B* **92** 045108
[23] Yu R, Weng H, Fang Z, Dai X and Hu X 2015 *Phys. Rev. Lett.* **115** 036807
[24] Yuan D, Yue C, Hu Y and Zhang W 2024 *Chin. Phys. Lett.* **41** 037304
[25] Wang Q, Zhang J, Huang J, Shi J, Zhang S, Guo H, Huang L, Ding H, Zhou W and Zhang Y F 2023 *Chin. Phys. B* **32** 016102
[26] Guo D L and Li H 2025 *Chin. Phys. B* **34** 067102
[27] Wu W, Liu Y, Li S, Zhong C, Yu Z M, Sheng X L, Zhao Y X and Yang S A 2018 *Phys. Rev. B* **97** 115125
[28] Soluyanov A A, Gresch D, Wang Z, Wu Q, Troyer M, Dai X and Bernevig B A 2015 *Nature* **527** 495
[29] Huang H, Zhou S and Duan W 2016 *Phys. Rev. B* **94** 121117
[30] Guo P J, Yang H C, Liu K and Lu Z Y 2017 *Phys. Rev. B* **95** 155112
[31] Bzdusek T, Wu Q, Ruegg A, Sigrist M and Soluyanov A A 2016 *Nature* **538** 75
[32] Ezawa M 2017 *Phys. Rev. B* **96** 041202
[33] Liu Z, Lou R, Guo P, Wang Q, Sun S, Li C, Thirupathaiah S, Fedorov A, Shen D, Liu K, Lei H and Wang S 2018 *Phys. Rev. X* **8** 031044
[34] Lou R, Guo P, Li M, Wang Q, Liu Z, Sun S, Li C, Wu X, Wang Z, Sun Z, Shen D, Huang Y, Liu K, Lu Z Y, Lei H, Ding H and Wang S 2018 *npj Quantum Mater.* **3** 43
[35] Yan Q, Liu R, Yan Z, Liu B, Chen H, Wang Z and Lu L 2018 *Nat. Phys.* **14** 461
[36] Zhao M, Zhuang Z Y, Wu F, Leng P, Joseph N B, Xie X, Ozerov M, He S, Chen Y, Narayan A, Liu Z and Xiu F 2024 *ACS Nano* **18** 16684
[37] Kohn W and Sham L J 1965 *Phys. Rev.* **140** A1133
[38] Hohenberg P and Kohn W 1964 *Phys. Rev.* **136** B864
[39] Kresse G and Furthmüller J 1996 *Phys. Rev. B* **54** 11169
[40] Kresse G and Hafner J 1993 *Phys. Rev. B* **47** 558
[41] Kresse G and Furthmüller J 1996 *Comput. Mater. Sci.* **6** 15
[42] Kresse G and Joubert D 1999 *Phys. Rev. B* **59** 1758
[43] Perdew J P, Burke K and Ernzerhof M 1996 *Phys. Rev. Lett.* **77** 3865
[44] Marzari N, Mostofi A A, Yates J R, Souza I and Vanderbilt D 2012 *Rev. Mod. Phys.* **84** 1419
[45] Mostofi A A, Yates J R, Pizzi G, Lee Y S, Souza I, Vanderbilt D and Marzari N 2014 *Comput. Phys. Commun.* **185** 2309
[46] Pizzi G, Vitale V, Arita R, *et al.* 2020 *J. Phys.: Condens. Matter* **32** 165902
[47] Wu Q, Zhang S N, Song H F, Troyer M and Soluyanov A A 2018 *Comput. Phys. Commun.* **224** 405
[48] Knappschneider A, Litterscheid C, Dzivenko D, Kurzman J A, Seshadri R, Wagner N, Beck J, Riedel R and Albert B 2013 *Inorg. Chem.* **52** 540
[49] Niu H, Wang J, Chen X Q, Li D, Li Y, Lazar P, Podloucky R and Kolmogorov A N 2012 *Phys. Rev. B* **85** 144116
[50] Guo P J, Yang H C, Zhang B J, Liu K and Lu Z Y 2016 *Phys. Rev. B* **93** 235142
[51] Ali M N, Xiong J, Flynn S, Tao J, Gibson Q D, Schoop L M, Liang T, Haldolaarachchige N, Hirschberger M, Ong N P and Cava R J 2014 *Nature* **514** 205
[52] Fu L, Kane C L and Mele E J 2007 *Phys. Rev. Lett.* **98** 106803
[53] Takane D, Wang Z, Souma S, Nakayama K, Trang C X, Sato T, Takahashi T and Ando Y 2016 *Phys. Rev. B* **94** 121108
[54] Xu Q, Yu R, Fang Z, Dai X and Weng H 2017 *Phys. Rev. B* **95** 045136